

**Solid State Nuclear Magnetic Resonance Studies of HydroxyPropylMethylCellulose Acetyl Succinate polymer, a Useful Carrier in Pharmaceutical Solid Dispersions.**

Andrea Pugliese<sup>a</sup>, Lucy E. Hawarden<sup>b</sup>, Anuji Abraham<sup>c</sup>, Michael Tobyn<sup>b</sup>, and Frédéric Blanc<sup>\*,a,d</sup>.

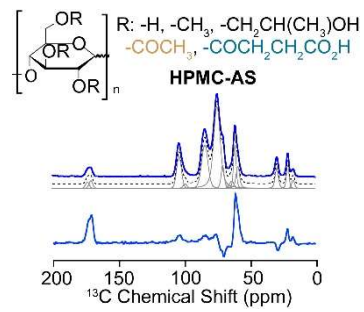
<sup>a</sup> Department of Chemistry, University of Liverpool, Crown Street, Liverpool L69 7ZD, UK.

<sup>b</sup> Bristol-Myers Squibb, Biopharmaceutics R&D, Reeds Lane, Moreton CH46 1QW, UK.

<sup>c</sup> Bristol-Myers Squibb, Drug Product Science and Technology, New Brunswick, New Jersey, 08903, US.

<sup>d</sup> Stephenson Institute for Renewable Energy, University of Liverpool, Peach Street, Liverpool L69 7ZF, UK.

## TOC



$^{13}\text{C}$  NMR spectral assignment of HPMC-AS is unambiguously obtained by step wise substitution and phase inversion NMR. (Semi)-quantitative  $^{13}\text{C}$  NMR is used to capture the grade-dependent A and S ratios.

## **ABSTRACT**

Hydroxypropylmethylcellulose acetyl succinate (HPMC-AS) is a key polymer used for the enablement of amorphous solid dispersions (ASDs) in oral solid dosage forms. Choice of the appropriate grade within the material is often made empirically, by the manufacturer of small scale formulations, followed by extensive real time stability. A key factor in understanding and predicting the performance of an ASD is related to the presence of hydrogen (or other) bonds between the polymer and active pharmaceutical ingredient (API), which will increase stability over the parameters captured by miscibility and predicted by the Gordon-Taylor equation. Solid state Nuclear Magnetic Resonance (NMR) is particularly well equipped to probe spatial proximities, for example between polymer and API, however in the case of HPMC-AS these interactions have been sometimes difficult to identify as the carbon-13 NMR spectra assignment is yet to be firmly established. Using feedstock, selectively substituted hydroxypropylmethylcellulose (HPMC) polymers and NMR editing experiments, we propose here a comprehensive understanding of the chemical structure of HPMC-AS and a definitive spectral assignment of the  $^{13}\text{C}$  NMR spectra of this polymer. The NMR data also captures the molar ratios of the acetate and succinate moieties present in HPMC-AS of various grades without the need for post treatment required by chromatography methods commonly use in pharmacopeia. This knowledge will allow the prediction and measurement of interactions between polymers and APIs, and therefore a rational choice of polymer grade to enhance the solid state stability of ASDs.

**Key words:** Solid-state NMR spectroscopy,  $^{13}\text{C}$ , hydroxypropylmethylcellulose, hydroxypropylmethylcellulose acetyl succinate, HPMC-AS, amorphous solid dispersion.

## INTRODUCTION

Active pharmaceutical ingredients (APIs) are often available in the thermodynamically stable crystalline form and exhibit poor water solubility,<sup>[1]</sup> hence poor bioavailability.<sup>[2]</sup> Amorphous drugs are therefore attractive due to their increased rate of dissolution enhancing the bioavailability of the active ingredient. However, their development is often hampered by their tendency to recrystallize to the most thermodynamically stable polymorph.

To address this challenge, several strategies based on formulation in polymers have been used to make amorphous solid dispersion (ASDs).<sup>[3]</sup> An ASD is a formulation of one or more API into a solid biocompatible polymer matrix that aims to stabilize the API in its amorphous form and increase bioavailability.<sup>[4]</sup> The most common methods to prepare ASDs include solvent evaporation,<sup>[5]</sup> spray drying,<sup>[6]</sup> cryo-milling,<sup>[7]</sup> hot melt extrusion,<sup>[8]</sup> nano-solid suspension formation using controlled precipitation,<sup>[9]</sup> and solvent-free supercritical fluid processing.<sup>[10]</sup> It is widely recognised that the polymer plays a crucial role in stabilising the ASD, and that the formulation of the API and polymer into a solid dispersion prevents API crystallisation and consequently improves physical stability.<sup>[11–13]</sup> This is mostly due to a synergetic effect that includes increase of the glass transition temperature ( $T_g$ ) of the final mixture high  $T_g$  polymers (anti-plasticising effect), reducing molecular mobility of the amorphous API and the formation of specific API-polymer interactions.<sup>[14]</sup>

A number of polymers have been considered as excipients in ASDs and can be classified as polyglycols (e.g., polyethylene glycol (PEG),<sup>[15]</sup> polyethylene oxide (PEO)<sup>[16]</sup>), polyvinyl (e.g., polyvinylpyrrolidone (PVP),<sup>[17]</sup> polyvinylpyrrolidone-polyvinyl acetate (PVP-VA)<sup>[18]</sup>) and cellulose (e.g., hydroxypropylmethylcellulose (HPMC),<sup>[19]</sup> hydroxypropylmethylcellulose acetyl succinate (HPMC-AS)<sup>[20]</sup>, Figure 1).

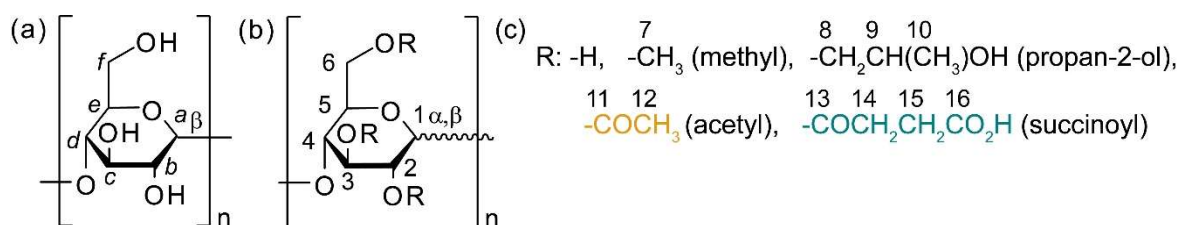


**Figure 1.** The pulp (a) is the chemical precursor of HPMC. The HPMC structure consists of the (b) 6-carbon ring unit of glucose bonded to hydrogen, methyl and propan-2-ol R groups given in (c). Esterification of HPMC yields HPMC-AS that is made from the glucose unit and all the substituent R groups in (c). HPMC-A and HPMC-S are made from the glucose unit and only the acetyl and succinoyl R groups, respectively. The wavy line in panel (b) represents the chemical bond of the anomeric carbon: the glucose ring exists in two different cyclic hemiacetal  $\alpha$ - and  $\beta$ - glucopyranose in which the anomeric carbon is a stereogenic centre and has two different configurations.

The choice of a suitable polymer to make a specific ASD is dictated by the chemical physical properties required such as  $T_g$ , thermal stability, the dissolution profiles in organic solvent, its performance in dissolve API as well as the API under consideration.

It has been described that HPMC-AS is a promising solid matrix for developing homogeneous amorphous dispersions<sup>[21]</sup> of low-solubility drugs due to its high glass temperature value ( $T_g$  is in order of 120 °C)<sup>[22]</sup> and its amphiphilic nature arising from

the existence of hydrophobic (e.g., succinoyl, Figure 1(b)) and hydrophilic (e.g. acetyl) groups in its chemical structure.<sup>[21]</sup>

Due to the presence of acetyl (A) and succinoyl (S) groups, HPMC-AS allows the formation of stable ASD and inhibition of the API crystallisation by the formation of intermolecular interactions.<sup>[23,24]</sup> A and S can establish specific interactions with the drug, that could be tuned by different levels of acetyl and succinoyl substitution in the polymers. Materials with different contents of A and S are commercially available and labelled as L, M and H grades depending on the A/S ratio according to the specifications given by different vendors.<sup>[25–27]</sup>

Solid-state Nuclear Magnetic Resonance (NMR) has been demonstrated as one of the most informative analytic technique used in the field of pharmaceutical sciences.<sup>[28,29]</sup> NMR allows the structural characterization of drugs<sup>[30]</sup> and excipients,<sup>[31]</sup> identification of drug polymorphs,<sup>[32]</sup> understanding of molecular mobility and physical stability of solid dispersions,<sup>[33]</sup> and the study and identification of specific intramolecular interactions in the solid dispersion.<sup>[34]</sup> The knowledge of the accurate assignments of the NMR signals in the HPMC-AS polymer used for ASDs plays a crucial role in understanding HPMC-AS – API interactions and is required to study the overall stability and dynamics of the ASD.

Many reports provide evidence of intermolecular interactions between API and polymer using computational, thermal and spectroscopic methods, reporting a partial NMR polymer assignments. The presence of hydrogen bonds in API-PVP solid dispersions has been probed by Fourier-Transform Infrared Spectroscopy (FT-IR), Raman and NMR spectroscopy, confirming ideal mixing behaviour of the two components.<sup>[35]</sup> Drug-polymer interactions between polystyrene sulfonic acid and lapatinib (LB) and gefitinib (GB) have been shown via the presence of acid-base interactions using a combination of analytic techniques, including solid-state NMR, ultraviolet (UV) spectroscopy and FT-IR.<sup>[36]</sup> Recently, a study by Ishizuka<sup>[23]</sup> and co-worker has probed intermolecular interactions between carbamazepine (CBZ) and HPMC-AS collating data obtained by studying CBZ in HPMC-A and CBZ in HPMC-S in individual solid dispersions. Without a complete assignment of the <sup>13</sup>C spectrum and only attributing the signal at ~170 ppm to the carbonyl of the acetyl group in HPMC-AS spectrum, the authors were able to identify the presence of intermolecular bonds between drug and HPMC-AS. In particular they have demonstrated the presence of a hydrogen bond between the acetate substituent of the polymer and the CBZ's amine group, and between both the carbonyl and amine groups of CBZ, proving the crucial role played by the acetate and succinoyl group in stabilization of the final solid dispersion. X. Lu *et al.*<sup>[24]</sup> detected specific intramolecular interactions in amorphous dispersions made by posaconazole (POSA), as API, and HPMC-AS and hypromellose phthalate (HPMC-P) at different API loading. They were able to identify interactions by combining one-, two-dimensional and advanced NMR techniques with isotopic labelling. The authors identified hydrogen bonding like interaction between the POSA's triazole ring and the –CH moiety of the propan-2-ol substituent group of HPMC-AS as well as an electrostatic like interaction between the triazole with the deprotonated succinoyl carboxylic group. π-π aromatic packing and electrostatic interactions were also detected between POSA and the HPMC-P polymer. In that paper, the authors also reported a preliminary assignment of the <sup>13</sup>C CP MAS NMR spectrum of HPMC-AS, however little details were given.

Here, we report a comprehensive NMR structural elucidation study of HPMC-AS, which provides an enhanced and more accurate assignment than those previously reported in

the literature in which the  $^{13}\text{C}$  NMR spectra of a range of common pharmaceutical excipients used in solid dispersion are described.<sup>[37]</sup> This is achieved by exploiting a stepwise approach relying on consecutive substitution of the HPMC polymer with acetate, succinate and a mixture of acetate and succinate moieties, combined with acquisition of well resolved and  $^1\text{H}$ -edited  $^{13}\text{C}$  NMR spectra and their thorough deconvolution. Additionally, it is demonstrated that it is possible to estimate the various contents of A and S directly from the experimentally obtained  $^{13}\text{C}$  NMR spectra to capture the different grade of HPMC-AS. These results could enable more effective identification of the presence of specific-site intermolecular interactions, pinpointing which organic functionalities are involved in specific interactions. In the specific case of HPMC-AS, this allows the possibility of tuning the A/S ratio in the sample to maximize the stabilization effect of the polymer on the final ASD.

## MATERIALS AND METHOD

### Materials

#### General considerations

Pulp polymer and HPMC were obtained from Shin-Etsu Chemical Co., Ltd. HPMC-AS polymers branded AQOAT<sup>®</sup>, AFFINSOL<sup>™</sup> and AQUASOLVE<sup>™</sup> with different acetate/succinate ratios were provided by Shin-Etsu Chemical Co, Ltd., DuPont Nutrition & Biosciences, and Ashland, respectively. Acetic anhydride and succinic anhydride (both 99% grade) used in the synthesis of HPMC-A and HPMC-S were obtained from Sigma-Aldrich. Acetic acid (99.8% grade), sodium acetate anhydrous (A.C.S. grade), and sodium chloride (reagent grade) were provided by Acros organic, Spectrum and Fisher, respectively. All other materials were used as received.  $^{13}\text{C}$  liquid state NMR spectra were obtained on a Bruker Avance 500 MHz spectrometer with the solvent peak as the internal reference. Melting points (m.p.) were measured using a Edu-Lab Melting Point Apparatus SRL MLTP 08019-200.

Table 1 gives the weight percentage contents of acetate (A) and succinate (S) in the HPMC-AS used in this work which are obtained from liquid chromatography methods as described in the United States/National Formulary and Japanese (USA-NF/JP) pharmacopeia and given in the certificate of analysis (CoA) provided by the vendors. The percentage contents in weight of A and S is then converted to degree of substitution (DS).<sup>[38]</sup>

**Table 1.** Degree of substitution (DS) of acetate (A) and succinate (S) moieties in the various HPMC-AS polymers studied here as a function of manufacturers and grade. A% and S% values are given by the vendor in the CoA and they represent wt%. DS (A) and DS (S) represent the degree of substitution of A and S in all polymers.

Polymer series:	AQOAT <sup>®</sup>			AFFINSOL <sup>™</sup>			AQUASOLVE <sup>™</sup>		
Grade:	L	M	H	L	M	H	L	M	H
A%:	7.9	9.1	11.5	8.1	9.6	11.6	8.1	10.8	13.6
S%:	14.8	11.0	7.4	15.1	11.3	6.9	16.3	11.4	6.0
DS(A):	0.18	0.21	0.27	0.19	0.22	0.27	0.19	0.25	0.32
DS(S):	0.14	0.11	0.07	0.15	0.11	0.07	0.16	0.11	0.06
DS(A)/DS(S):	1.3	1.9	3.6	1.3	2.0	3.9	1.2	2.2	5.3

### Synthesis of HPMC-A

In a 500 mL 2-neck round bottom flasks equipped with a reflux condenser, HPMC (2910) (30.0 g, 94 mmol) was added to glacial acetic acid (300 mL) at 80-90 °C under mechanical vigorous stirring using a Teflon stir blade over 1-2 minutes. Upon HPMC dissolution, anhydrous sodium acetate (30.0 g, 365 mmol) was added and stirred until completely dissolved which was followed by addition of acetic anhydride (66.34 g, 650 mmol) over 5 minutes. The resulting mixture was then stirred at a moderate speed (200-250 rpm) for 6 hours at 80-90 °C and was quenched by pouring it into 10% NaCl solution in water (1.4 L). The resulting precipitate was collected by filtration and then suspended in fresh 10% NaCl (0.7 L) in a laboratory blender and mixed until well dispersed (1-2 minutes). The precipitate was again collected by filtration, re-suspended a second time in 10 % NaCl solution, dispersed then re-collected by filtration. After drying, the wet-cake was purified by three washes in hot distilled water (0.7 L each) at 70-80 °C. Finally, the precipitate was placed in an 80 °C oven to dry, leading a white granular solid (25.5 g). <sup>13</sup>C NMR (125 MHz, DMSO-d<sub>6</sub>): 169.4 ppm, 169.2, 168.9, 168.4, 101.3, 99.1, 83.3, 82.6, 81.3, 79.7, 76.5, 75.1, 74.9, 74.8, 74.0, 73.5, 73.0, 71.8, 71.5, 70.3, 69.0, 68.9, 65.1, 64.9, 62.5, 59.3, 58.9, 58.8, 58.7, 58.5, 58.1, 57.6, 57.4, 55.4, 20.4, 20.1, 19.9, 19.8, 16.0. All peaks are broad. m.p.: 184 °C - 214 °C. Integration of the acetate carbonyls to the anomeric carbon of the glucose ring gave an acetate DS of 0.60.

### Synthesis of HPMC-S

In a 500 mL 2-neck round bottom flasks equipped with a reflux condenser, HPMC (2910) (30.0 g, 94 mmol) was dissolved under vigorous mechanical stirring in glacial acetic acid (300 mL) at 80-90 °C. When the mixture appears to be clear, anhydrous sodium acetate (30.0 g, 365 mmol) was added under vigorous stirring followed by succinic anhydride (3.51g, 33 mmol) and the reaction mixture was left at 80-90 °C for 6 hours. After cooling down to room temperature overnight, the polymer was isolated by pouring the crude into a 20% NaCl solution in water (1.5 L) followed by filtration. The precipitate was suspended twice in fresh 20% NaCl solution (0.7 L) in a laboratory blender mixing at the high speed for 1-2 minutes, and collected by filtration. The wet-cake was dissolved in 1.0 L of distilled water and then heated to 80-90 °C while stirring. The polymer began to phase separate as an off-white solid precipitate that was collected to lead the final product (18.6 g of yellowish solid) after drying. <sup>13</sup>C NMR (125 MHz, DMSO-d<sub>6</sub>): 172.5 ppm, 171.2, 171.0, 170.3, 169.5, 169.2, 102.2, 101.6, 101.3, 83.4, 82.6, 79.8, 77.9, 76.5, 75.1, 74.9, 74.1, 73.5, 73.0, 71.9, 70.5, 69.1, 65.1, 64.8, 62.6, 59.3, 58.8, 58.1, 28.8, 28.4, 20.4, 20.0, 19.7, 19.5, 18.9, 16.7, 16.1. All peaks are broad. m.p.: 204 °C – 234 °C. Integration of the acetate carbonyls to the anomeric carbon of the glucose ring gave an acetate DS of 0.15.

### NMR spectra

All solid state NMR spectra were acquired at 9.4 T using a Bruker Avance III HD NMR spectrometer equipped with a 4 mm HXY triple-resonance MAS (magic angle spinning) probe in double resonance mode. <sup>1</sup>H and <sup>13</sup>C channels were tuned at  $\nu_0 = 400.13$  MHz and 100.67 MHz respectively. All experiments were performed under MAS at a frequency  $\nu_r = 12.5$  kHz and at room temperature (298 K). All <sup>1</sup>H pulses and SPINAL-64 heteronuclear decoupling<sup>[39]</sup> during <sup>13</sup>C detection were obtained at a radio frequency (rf) field amplitude of 83 kHz. The <sup>1</sup>H-<sup>13</sup>C Cross Polarisation (CP) spectra<sup>[40]</sup> were carried out using a <sup>13</sup>C rf field amplitude of around 45 kHz ramped to obtain maximum signal at

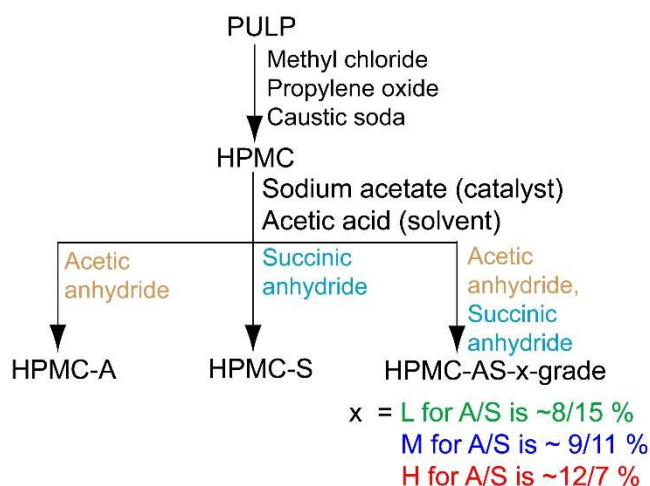
a  $^1\text{H}$  rf field of 60 kHz. A 2 ms contact time during CP was applied. Based on the  $^1\text{H}$  spin-lattice relaxation times,  $T_1$ , values, evaluated using the saturation recovery pulse sequence, recycle delays of 3 s were used in all the experiments.<sup>[41]</sup>  $^{13}\text{C}$  Cross-Polarisation Phase Inversion (CPPI)<sup>[42]</sup> experiments were performed using an optimised polarisation inversion period of 60  $\mu\text{s}$ . All  $^{13}\text{C}$  spectra were referenced to the tertiary carbon of adamantane at 29.45 ppm.<sup>[43]</sup> The chemical shifts of all assigned resonances are quoted within an accuracy of  $\pm 1$  ppm due to the broad line widths observed. Deconvolution of the experimental spectra was carried out in TopSpin 4.0.6 using the SOLA (Solid Line Shape Analysis) routine. Deconvolution for signals in the 160 and 190 ppm region were carried out using a fixed ratio for Lorentzian to Gaussian line shape of 1:6. The values for the  $^{13}\text{C}$  CP kinetics from the signal intensity vs CP contact time build up curve were obtained by fitting the relative datasets using the eq. 1 reported in the literature,<sup>[40]</sup> where  $S(t_c)$ ,  $S_0$ ,  $t_c$ ,  $T_{\text{HX}}$ , and  $T_{1\rho}$  are the amount of signal at time  $t_c$ , the maximum obtainable intensity in absence of relaxation, the contact time, the time constant for CP and the relaxation time in the rotating frame, respectively.

$$S(t_c) = S_0 \left[ 1 - \exp\left(\frac{-t_c}{T_{\text{HX}}}\right) \right] \exp\left(\frac{-t_c}{T_{1\rho}}\right) \quad \text{Eq. 1}$$

The first term of this equation accounts for the polarisation build up while the second exponential term accounts for the relaxation decay.

## RESULTS AND DISCUSSION

HPMC-A and HPMC-S differ for the presence of only acetate and succinate groups, respectively, bonded to the 6-carbon ring unit of cellulose (Figure 1(a)). HPMC-AS is prepared by esterification of HPMC with a mixture of acetic acid anhydride and succinic acid anhydride in acetic acid and sodium acetate.<sup>[44]</sup> The mono-esterified derivatives HPMC-A (hydroxypropylmethylcellulose acetate) and HPMC-S (hydroxypropylmethylcellulose succinate) (Figure 1) are also prepared from HPMC using acetic and succinic acid anhydrides, respectively, as summarised in Scheme 1.



**Scheme 1.** Synthetic pathway in which the pulp, as starting material, was transformed in the samples used in this work.

The pulp (also referred as cellulose) consists of a polysaccharide constituted linear chain of  $\beta$ -1,4-linked D-glucose residues, and exhibits complexity at the molecular level.<sup>[45]</sup> Cellulose is an allomorphic material composed of two native crystalline forms (cellulose I  $\alpha$  and  $\beta$ ), another allomorphic form (cellulose II) and an amorphous phase<sup>[45]</sup> and the chemical structure of the polymeric unit is given in Figure 1(a). Figure 2(a) shows the  $^{13}\text{C}$  CP MAS spectrum of the pulp with the assignment proposed based on the previous literature, supported by both experimental data<sup>[46]</sup> and computational study.<sup>[47]</sup> The spectrum exhibits clusters of signals for *Ca*, *Cb,c,e*, *Cd* and *Cf* at 104 - 108 ppm, 70 - 78 ppm, 82 - 90 ppm and 60 - 68 ppm, respectively, arising from the presence of allomorphic and amorphous forms of cellulose. Figure 2(b) also gives the  $^{13}\text{C}$  CP-based edited experiment we have recorded using the CPPI sequence (in which the phase of the signals depends on the carbon types with quaternary carbon and  $\text{CH}_3$  signals being positive,  $\text{CH}_2$  negative and  $\text{CH}$  signals largely suppressed).<sup>[48]</sup> In the  $^{13}\text{C}$  CPPI spectrum, the intensity of *Ca*, *Cd*, *Cb,c,e* peaks is highly reduced as expected for  $\text{CH}$  moieties and partial inversion is only observed for the *Cf* cluster ( $\text{CH}_2$  group), likely originating from different spin dynamics between the various forms.<sup>[45]</sup>

The assignment of the  $^{13}\text{C}$  CP MAS spectrum can be used for stepwise assignment of all the samples studied in this work, as the pulp is the chemical precursor of all the polymers used (Scheme 1).

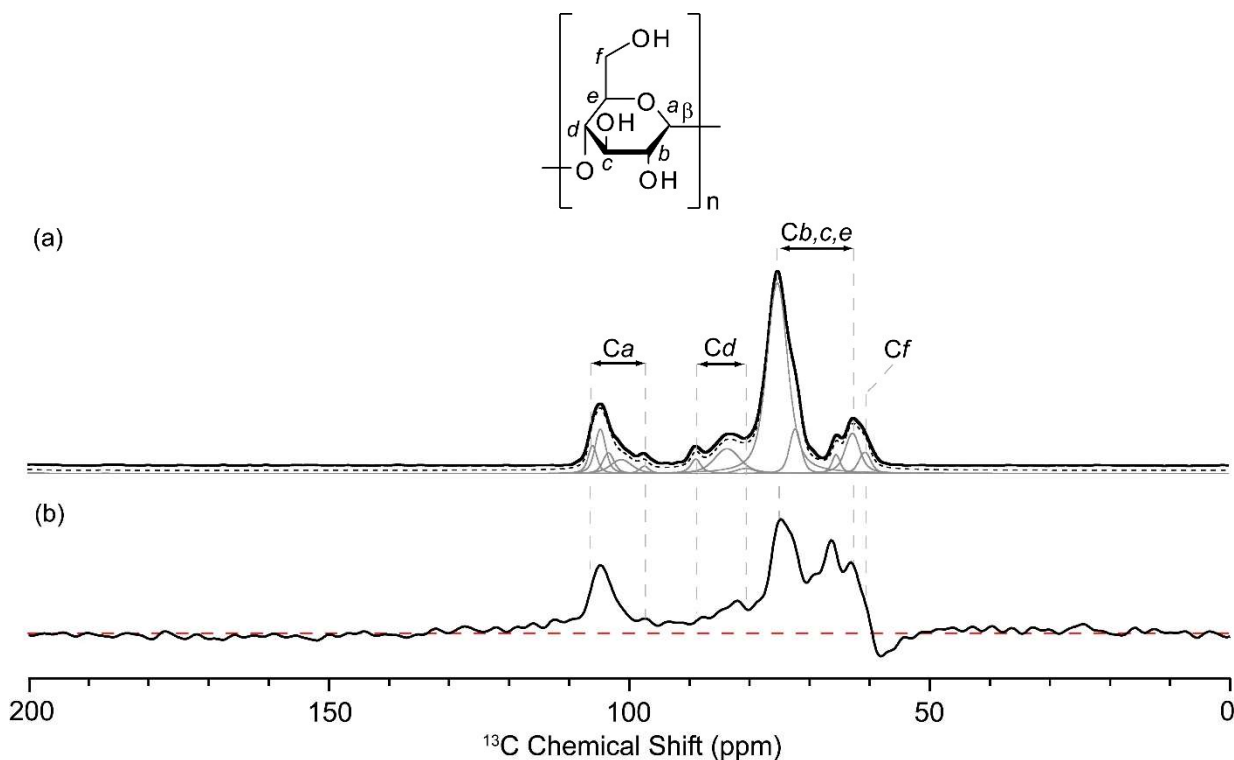


**Figure 2.** (a)  $^{13}\text{C}$  CP MAS and (b)  $^{13}\text{C}$  CPPI MAS spectra of pulp and its chemical structure. The proposed assignments are based on the previous literature.<sup>[46,47]</sup> The simulated spectrum (dashed black) and the spectral deconvolution (grey line) is given. The red dotted line in (b) marks the zero intensity signal.

The assignment of the  $^{13}\text{C}$  MAS NMR spectra of HPMC-AS is initially based on the partial spectral assignment of unsubstituted HPMC. The  $^{13}\text{C}$  CP spectrum of HPMC is shown in Figure 3(a) and its assignment is based on comparisons with previous  $^{13}\text{C}$  NMR spectra of excipients and carbohydrates,<sup>[37]</sup> well-established understanding of  $^{13}\text{C}$  chemical shielding<sup>[49]</sup> including computed shifts, prior literature,<sup>[37,50]</sup> and a  $^{13}\text{C}$  CP-based edited experiment given in Figure 3b using the CPPI sequence. The  $^{13}\text{C}$  spectrum of HPMC clearly exhibits two signals at around 104 and 98 ppm, corresponding to the two different anomeric C1 $\alpha$  and C1 $\beta$  (Figure 1(a)) which appear at two chemical shifts due to the different electronic distribution at the anomeric centres.<sup>[51]</sup> The peaks at 84 and 76 ppm correspond to C4 and C2,3, respectively. The intense peak at 61 ppm, that is significantly reduced in the  $^{13}\text{C}$  CPPI spectrum, can be attributed to the CHs' C5,9. Spectral deconvolution reveals shoulders at about 71 and 59 ppm that appear negative and positive in the  $^{13}\text{C}$  CPPI spectrum and are assigned to the CH<sub>2</sub>s' C6,8 and methyl C7, respectively. We note that the previous partial  $^{13}\text{C}$  spectral assignment indicates the 71 and 61 ppm signals (appearing at 75 and 60 ppm in the literature)<sup>[37]</sup> to correspond to C2,3,5,9 and C6,7,8, respectively, and this is not in agreement with the negative phase for CH<sub>2</sub>s groups and reduced signal intensities for CHs groups observed in the  $^{13}\text{C}$  CPPI spectrum (Figure 3(b)).

The small signal labelled as C6<sup>u</sup> (where 'u' means unsubstituted) in the spectra at about 67 ppm is tentatively attributed to carbon C6 in the glucose unit corresponding to some residual unsubstituted hydroxyl group,<sup>[52]</sup> this assignment is based on the chemical shift observed for the carbon Cf of the pulp (Figure 2(a) and (b)).<sup>[44,45]</sup> It is estimated that around 20% of hydroxyl groups in HPMC are unsubstituted by methoxy and

hydroxypropyl groups.<sup>[52]</sup> These residual groups are subsequently reacted during the synthesis of HPMC-AS.

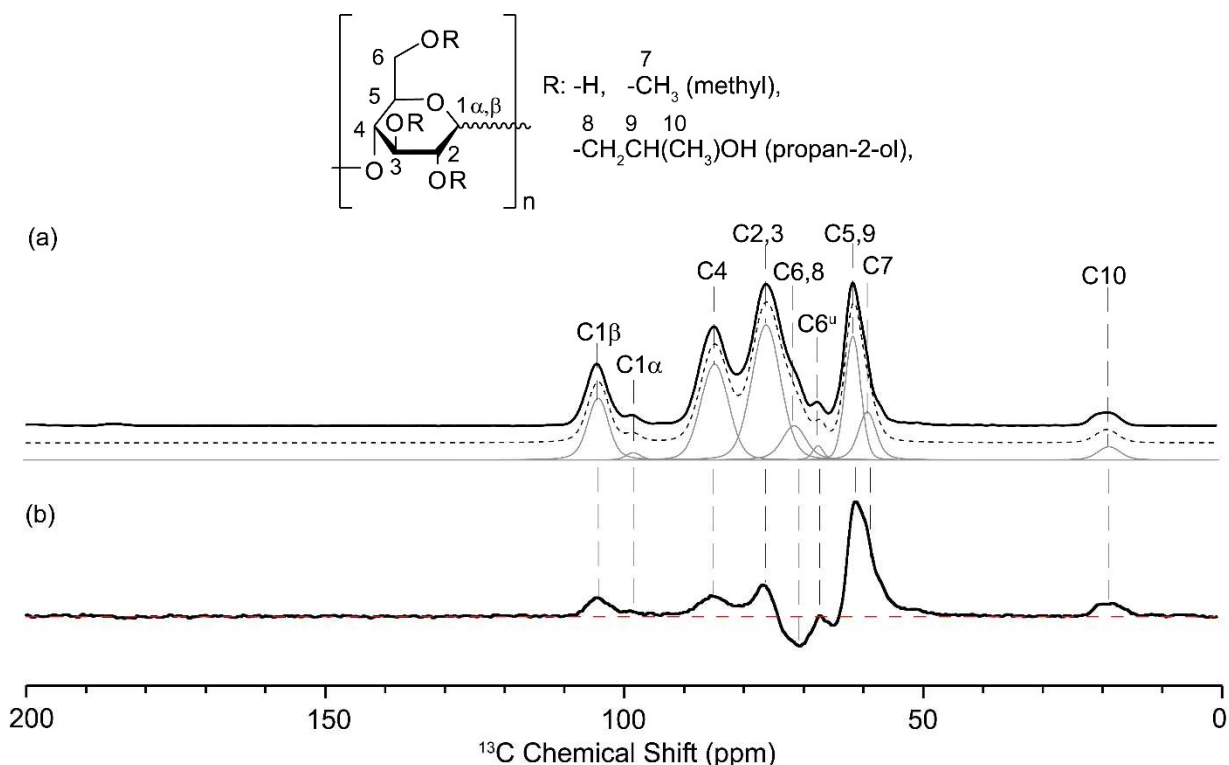


**Figure 3.** (a) <sup>13</sup>C CP MAS and (b) <sup>13</sup>C CPPI MAS spectra of HPMC and its chemical structure. The simulated spectrum (dashed black) and the spectral deconvolution (grey line) are given for the CP spectrum. The red dotted line in (b) marks the zero intensity signal.

In order to unambiguously assign the <sup>13</sup>C CP MAS NMR spectra of HPMC-AS, we also recorded the spectra of HPMC-A and HPMC-S polymers prepared by esterification of HPMC (see synthesis section for further details). The respective <sup>13</sup>C NMR spectra of these polymers (Figures 4(a) and (b)) differ from the spectrum of HPMC (Figure 3(a)) by the presence, in HPMC-A, of two extra peaks at 170 and 21 ppm corresponding to the carbonyl (C11) and methyl groups (C12) of the acetyl, respectively, and, in HPMC-S, of resonances at 173 and 30 ppm of the carbonyl (C13,16) and methylene (C14,15) carbons of the succinoyl group. We were unable to resolve the two different carbonyls (ester C13 and carboxylic acid C16) of the succinoyl group, despite the expected 3-4 ppm difference in solution state<sup>[49]</sup> which is ascribed to signal broadening of the 173 ppm resonance (full width at half maximum ~ 500 Hz vs. 250 Hz for C11 in HPMC-A).

The signal assignment for the HPMC-AS AQOAT<sup>®</sup> series (Figure 4(c, d1, and e)) was carried out using assignments obtained for HPMC, HPMC-A, and HPMC-S and the <sup>13</sup>C CPPI spectrum obtained on HPMC-AS M grade given in Figure 4(d2). The spectra exhibit resonances for both the acetyl and succinoyl groups in addition to the signals that come from HPMC. The carbonyl carbons of the acetyl (C11) and succinoyl (C13,16) groups are partially resolved, enabling their (semi)quantification (see below). Similarly, in the aliphatic region of the spectra, resonances for the acetyl (C12 at 21 ppm) and succinoyl (C14,15 at 30 ppm) groups as well as the C10 in HPMC are clearly visible.

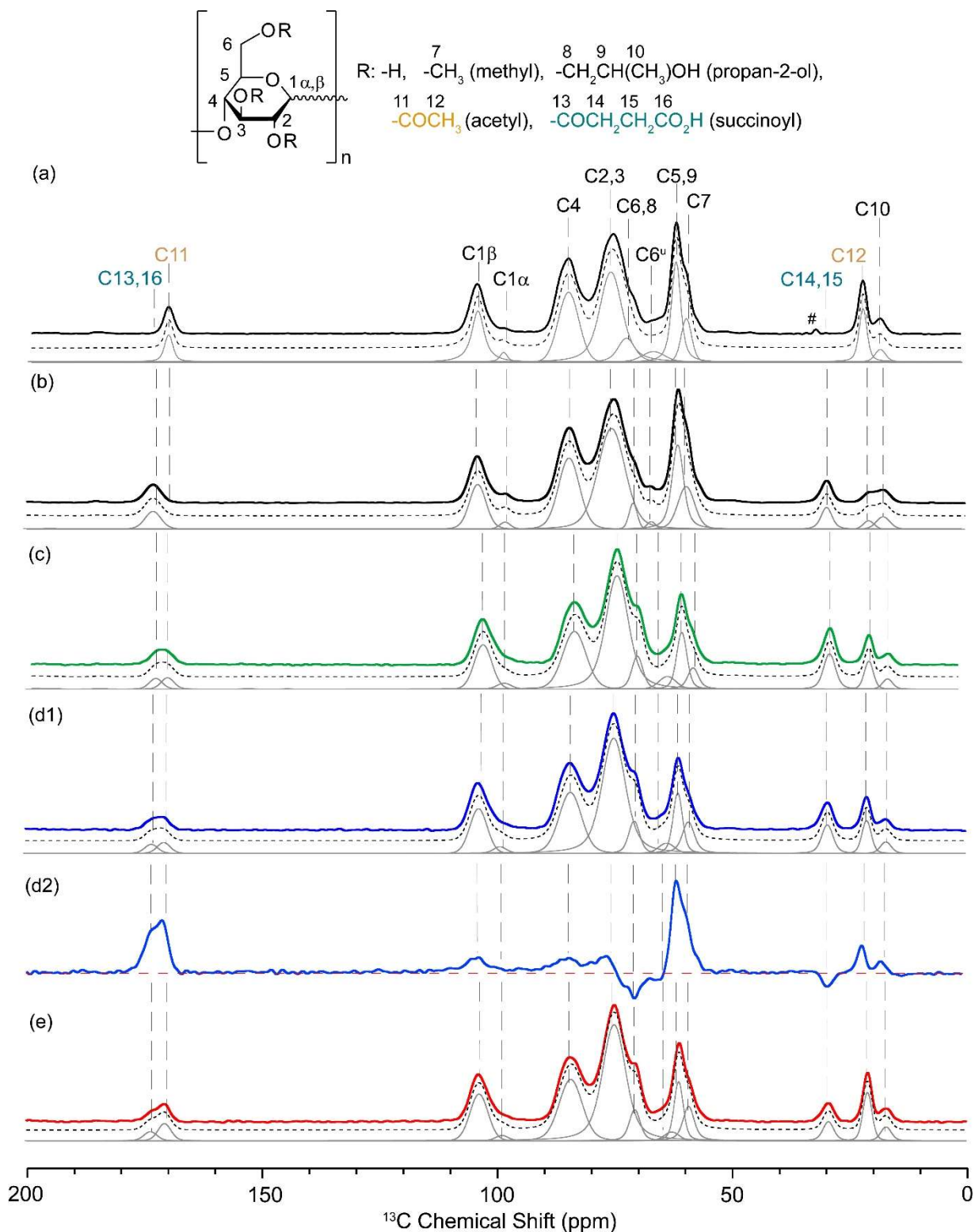


**Figure 4.**  $^{13}\text{C}$  CP MAS spectra of (a) HPMC-A, (b) HPMC-S and Shin-Etsu AQOAT<sup>®</sup> HPMC-AS in (c) L-, (d1) M-, and (e) H-grades. The  $^{13}\text{C}$  CPPI spectra of Shin-Etsu HPMC-AS-M polymer is given in (d2). The red dotted line marks the zero intensity signal. The simulate spectrum (dashed black) and the spectral deconvolution (grey line) are given for each spectrum. The signal at 31 ppm (labelled with #) indicates some acetate present in the sample due to transesterification with acetic acid solvent during the synthesis. The structure of HPMC-AS polymer is shown on the top of the figure.

Figures 5 and 6 show the  $^{13}\text{C}$  CP MAS NMR spectra obtained for HPMC-AS AFFINISOL<sup>TM</sup> and AQUASOLVE<sup>TM</sup> polymers, respectively. The signals are comparable to the AQOAT<sup>®</sup> series and are assigned in the same way. Some small changes in chemical shifts were observed (Table 2) between the samples from different vendors rather than samples of different A/S ratio, further confirming that the carbon chemical shifts are not A/S ratio dependent.

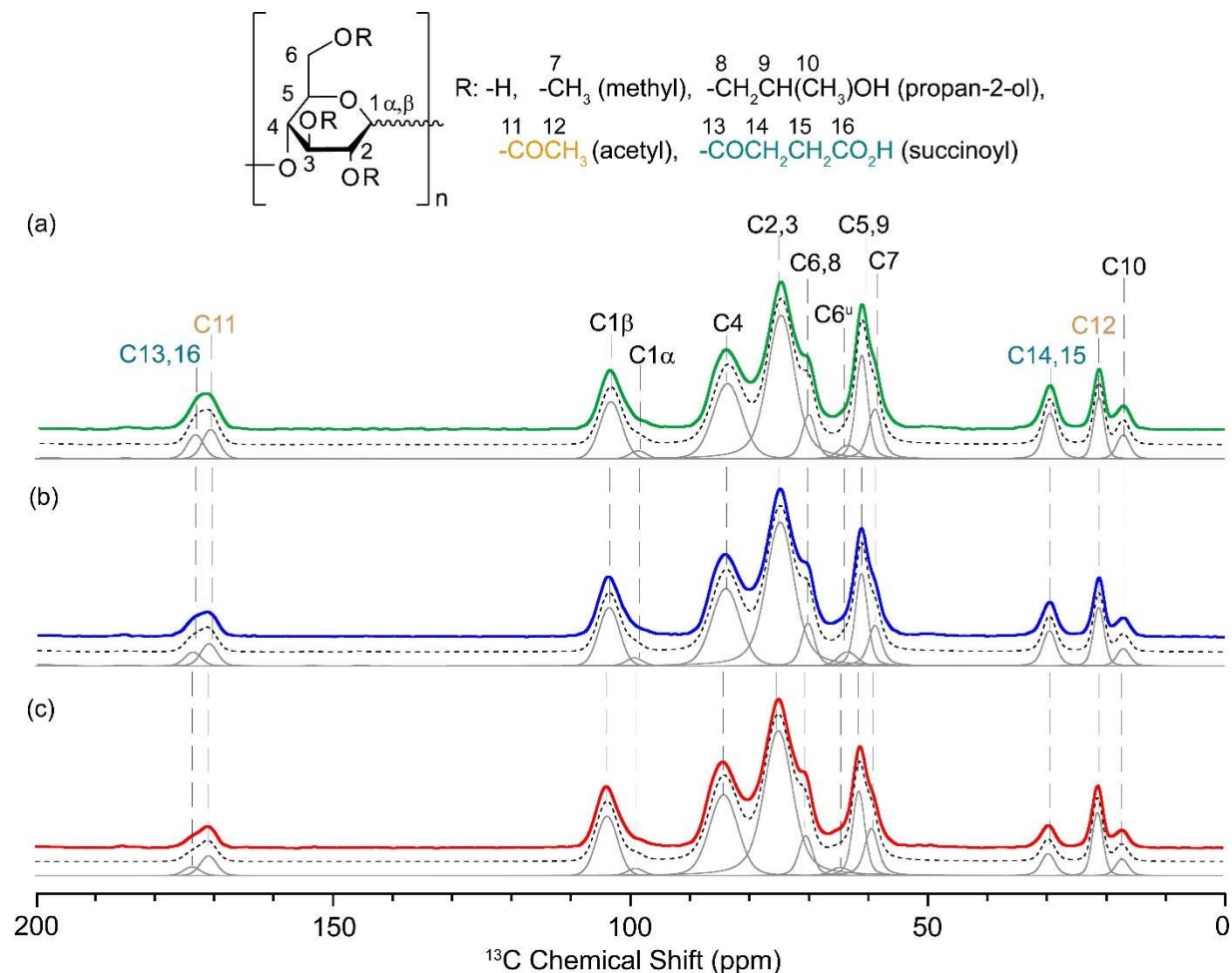


**Figure 5.**  $^{13}\text{C}$  CP spectra of the DuPont AFFINISOL<sup>TM</sup> HPMC-AS series at (a) L-grade, (b) M-grade, and (c) H-grade of acetyl/succinoyl ratio. The simulated spectrum (dashed black) and the spectral deconvolution (grey line) are given for each spectrum. The structure of HPMC-AS polymer is shown on the top of the figure.

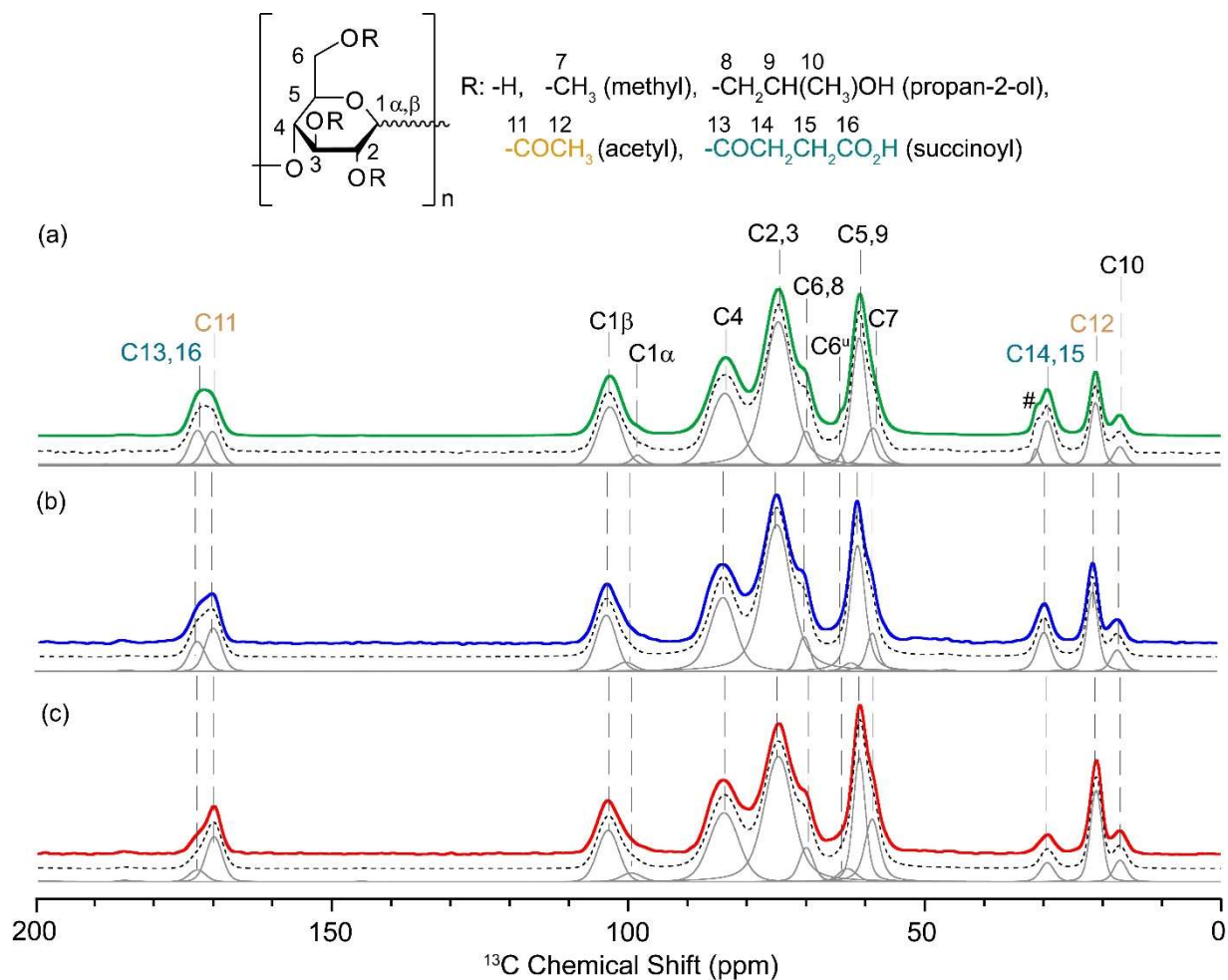


**Figure 6.** <sup>13</sup>C CP spectra of the Ashland AQUASOLVE™ at (a) L-grade, (b) M-grade, and (c) H-grade of acetyl/succinoyl ratio are reported. The simulated spectrum (dashed black) and the spectral deconvolution (grey line) are given for each spectrum. The signal labelled with # indicates the presence of some acetate in the sample due to transesterification with acetic acid solvent. On the top of the figure, HPMC-AS chemical structure is given.

**Table 2.** <sup>13</sup>C NMR spectral assignments chemical shifts in ppm for all polymers studied.

Polymer	C1 $\alpha$	C1 $\beta$	C2	C3	C4	C5	C6	C7	C8	C9	C10	C11	C12	C13	C14	C15	C16
HPMC	104(/)	98(/)	76(/)	76(/)	84(/)	61(+)	71(-)	59(+)	71(-)	61(+)	19(+)	n.a.	n.a.	n.a.	n.a.	n.a.	n.a.
HPMC-A	104	98	76	76	84	61	71	59	71	61	17	170	21	n.a.	n.a.	n.a.	n.a.
HPMC-S	104	98	76	76	84	61	71	59	71	61	17	n.a.	n.a.	173	30	30	173
AQOAT <sup>®</sup>	104(/)	98(/)	76(/)	76(/)	84(/)	61(+)	71(-)	59(+)	71(-)	61(+)	14(+)	171(+)	21(+)	173(+)	30(-)	30(-)	173(+)
AFFINISOL <sup>™</sup>	104	98	75	75	84	60	71	59	71	61	17	171	21	173	30	30	173
AQUASOLVE <sup>™</sup>	104	100	75	75	84	60	71	58	71	60	17	171	21	173	29	29	173

n.a. = not applicable. (+), (-) and (/) refer to the positive phase, negative phase and largely suppressed signal intensities for the <sup>13</sup>C CPPI spectra on selected polymers.

Although CP MAS NMR experiments are inherently not quantitative, the similar structure of the HPMC-AS polymers allows some (semi)quantitative consideration of the various groups present. The signals for carbons C11 (in A) and C16,13 (in S) were used as probes to quantify the A/S molar ratio from the experimental spectra as both these carbonyl carbons exhibit similar CP kinetics, which is very different than the one for either C12 (in A) or C14,15 (in S) due to the different nature of these carbons (CH<sub>3</sub> vs. CH<sub>2</sub> groups, respectively). The differences in CP kinetics are due to competing effects between the strength of the <sup>1</sup>H <sup>13</sup>C heteronuclear dipolar couplings and the different relaxation rates induced by different <sup>13</sup>C CP polarising build up curves for different kinds of carbons.<sup>[40]</sup> <sup>13</sup>C CP MAS spectra at different CP contact times were collected (selected spectra are given in Figure 7(a)) in order to demonstrate that the most representative carbons to use for the (semi)quantitative quantification of the DS(A)/DS(S) are the quaternary carbon C11 for the A unit and the quaternary carbon C13,16 for the S unit. The <sup>13</sup>C CP polarising build up curves (signal intensities vs. CP contact times) and fitting data (see experimental section for the equation)<sup>[40]</sup> are provided in Figure 7(b) and Table 3, clearly illustrating that C11 (gold, x) and C13,16 (dark green, ■) exhibit a similar CP kinetics which is significantly different than for C12 and C14,15, hence disqualifying them for the (semi)quantification.

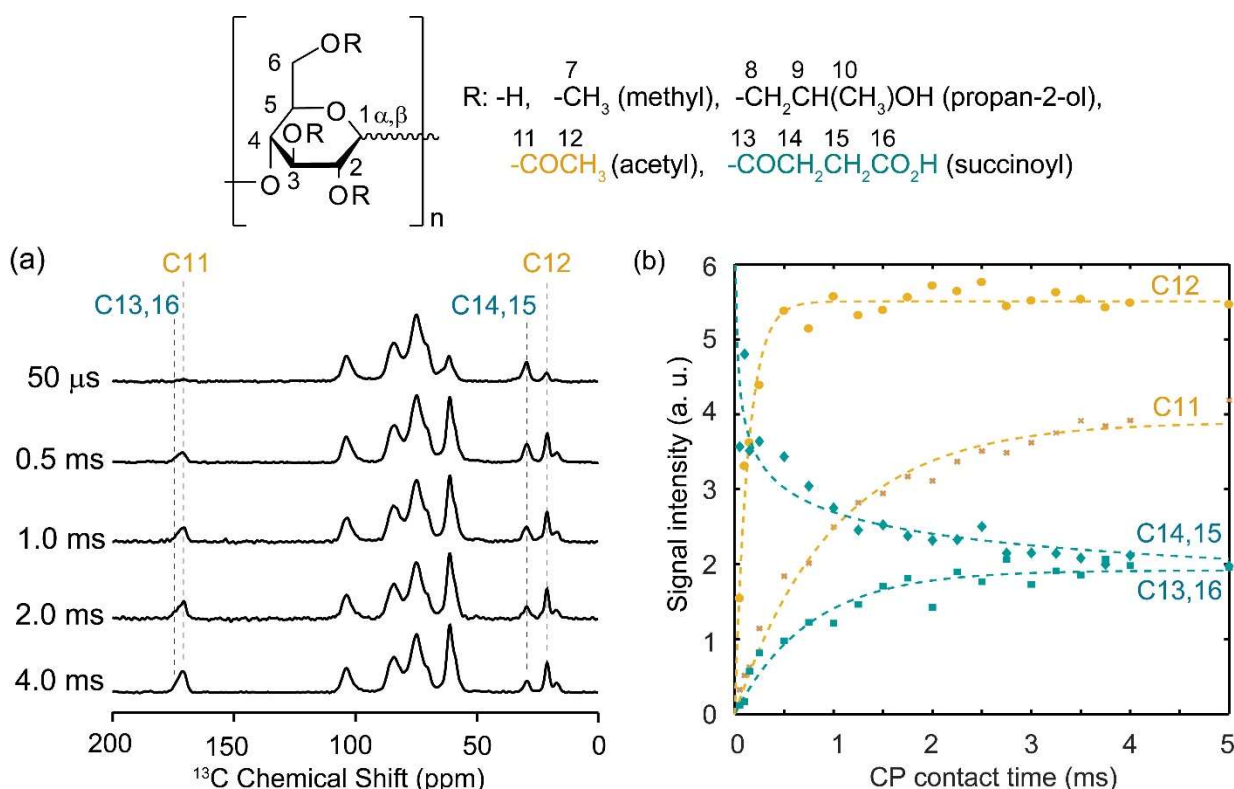


**Figure 7.** (a) <sup>13</sup>C CP MAS NMR spectra of the Shin-Etsu AQOAT<sup>®</sup> HPMC-AS M-grade polymer recorded at selected CP contact times (and its structure). (b) <sup>13</sup>C CP polarising build up curves (CP kinetics) for C11, C12, C13,16 and C14,15 carbons. The dashed lines are fit to the data using equation 1 (see experimental section).<sup>[40]</sup>

**Table 3.**  $^{13}\text{C}$  CP polarising build up curves fitting parameters for equation 1 for the ShinEtsu AQOAT<sup>®</sup> HPMC-AS M-grade polymer. See experimental section for further details.

Carbon	$S_0$	$T_{HX}$ (ms)	$T_{1\rho}$ (ms)
C11	$3.9 \pm 0.4$	$1.0 \pm 0.2$	n.d.
C12	$5.9 \pm 0.4$	$0.2 \pm 0.1$	n.d.
C13,16	$1.9 \pm 0.4$	$0.8 \pm 0.2$	n.d.
C14,15	$-0.2 \pm 0.3$	n.d.	$0.03 \pm 0.02$

n.d. = not determined

Figure 8 shows a magnified view of the signals related to the carbonyl groups of the acetate and succinate (190 – 160 ppm region of the  $^{13}\text{C}$  CP MAS NMR spectra). The spectra show different integrals for the characteristic C11 resonance in the A group and the C13,16 signals in the S group and allow comparison between vendors and grades. The different A/S molar ratios in each polymer can be obtained from the NMR integrals. It is found that for each vendor, the ratio DS(A)/DS(S) increases from the L to M to H nominal grade polymers (Table 1) which is in agreement with the increase in acetate content. The molar ratios found between these functional groups by NMR closely reflects the DS ratios determined by liquid chromatography and captured in the relevant certificates of analysis (Table 4).

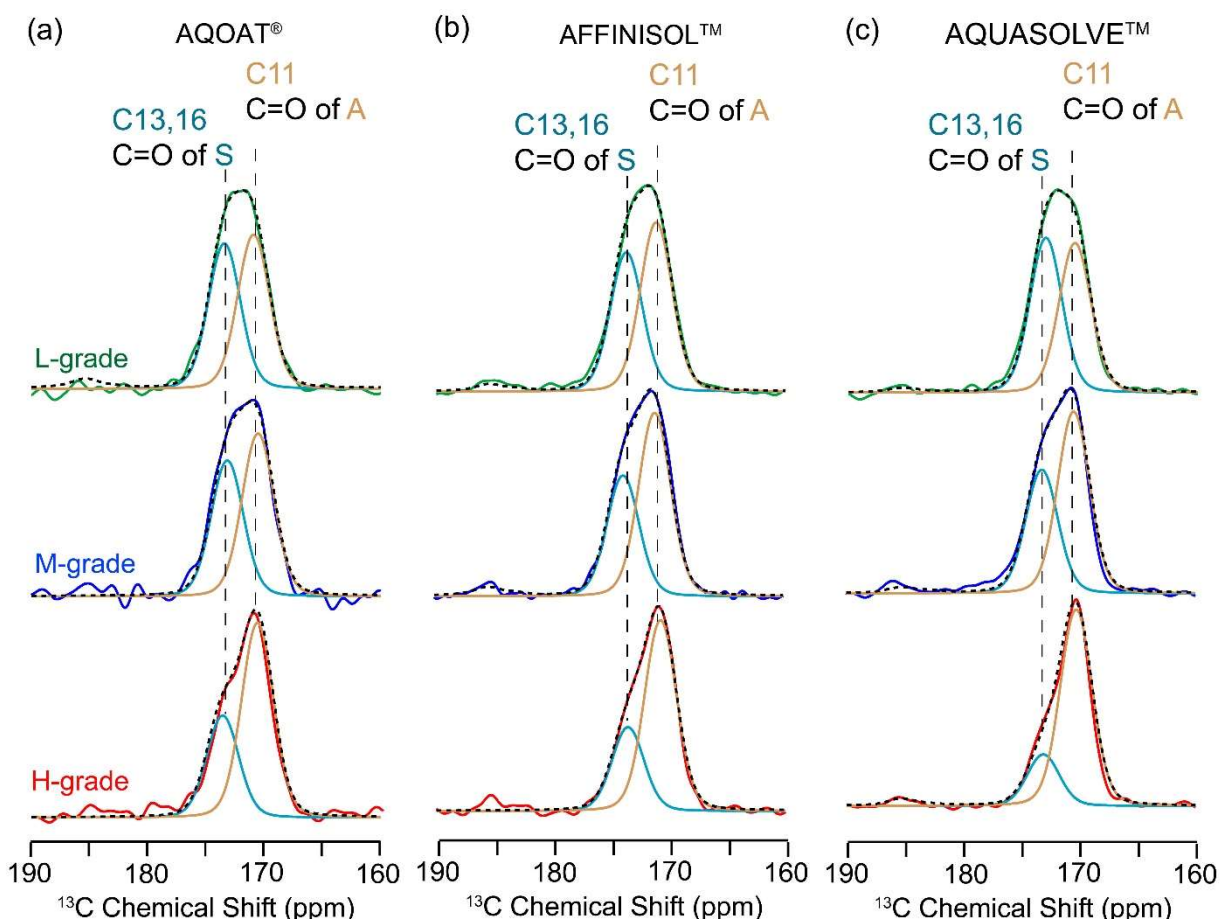


**Figure 8.** Magnified view of the 190 – 160 ppm region for HPMC-AS polymers as function of the grades for the (a) AQOAT<sup>®</sup>, (b) AFFINISOL<sup>™</sup> and (c) AQUASOLVE<sup>™</sup> series. Signals arising from the succinoyl and acetyl groups are given in turquoise and gold, respectively.

**Table 4.** Estimated mol A/S ratio values obtained experimentally from NMR, using the integrals for C16,13 and C11 as discussed in the text. The nominal DS A/S ratios obtained from liquid chromatography are given in brackets (see Table 1).

	AQOAT <sup>®</sup>	AFFINISOL <sup>™</sup>	AQUASOLVE <sup>™</sup>
L-grade	$2.0 \pm 0.1$ (1.3)	$2.4 \pm 0.1$ (1.3)	$2.1 \pm 0.1$ (1.2)
M-grade	$2.4 \pm 0.1$ (1.9)	$3.2 \pm 0.2$ (2.0)	$3.1 \pm 0.1$ (2.2)
H-grade	$3.6 \pm 0.6$ (3.6)	$4.5 \pm 0.1$ (3.9)	$7.5 \pm 0.2$ (5.3)

## CONCLUSION

We have presented a structural elucidation of the different grades of HPMC-AS, containing different acetyl and succinoyl contents and its precursors using <sup>13</sup>C CP MAS NMR and <sup>13</sup>C edited spectra, and refined the published spectral assignment. We demonstrated that this approach allows an estimation of the molar ratio of both groups and complements the liquid chromatography method used in the field. The knowledge of the structure and dependency of the <sup>13</sup>C chemical shifts on the local chemical environments will allow spatial interactions between this polymer and APIs to be detected and understood in ASDs. The work illustrates that the complexity of the HPMC-

AS structure requires access to  $^{13}\text{C}$  CP MAS NMR spectra and knowledge of  $^{13}\text{C}$  chemical shifts of each specific batch of polymer to ensure that any change in chemical shifts in the ASDs are precisely captured.

### **ACKNOWLEDGEMENTS**

AP thanks Bristol-Myers Squibb and the Engineering and Physical Science Research Council (EPSRC) for a PhD studentship under the scheme of National Productivity Investment Fund (NPIF) (EP/R51231X/1). We also thank S. Warashina (Shin-Etsu) and M. Brackhagen (DuPont) for the fruitful discussion about NMR assignments and materials. We also thank W. Miller, J. Cape, and A. Pluntze (Lonza Pharma & Biotech) for preparing HPMC-A and HPMC-S.

## REFERENCES

- [1] L. Carpentier, R. Decressain, A. De Gusseme, C. Neves, M. Descamps, *Pharm. Res.* **2006**, *23*, 798–805.
- [2] R. O. Williams, M. Zhang, H. Li, B. Lang, K. O'Donnell, H. Zhang, Z. Wang, Y. Dong, C. Wu, *Eur. J. Pharm. Biopharm.* **2012**, *82*, 534–544.
- [3] S. Baghel, H. Cathcart, N. J. O'Reilly, *J. Pharm. Sci.* **2016**, *105*, 2527–2544.
- [4] G. Van Den Mooter, J. Van Den Brande, P. Augustijns, R. Kinget, *J. Therm. Anal.* **1999**, *57*, 493–507.
- [5] K. J. Crowley, G. Zografi, *Pharm. Res.* **2003**, *20*, 1417–1422.
- [6] H. Takeuchi, S. Nagira, H. Yamamoto, Y. Kawashima, *Int. J. Pharm.* **2005**, *293*, 155–164.
- [7] K. J. Crowley, G. Zografi, *J. Pharm. Sci.* **2002**, *91*, 2150–2165.
- [8] Z. Dong, A. Chatterji, H. Sandhu, D. S. Choi, H. Chokshi, N. Shah, *Int. J. Pharm.* **2008**, *355*, 141–149.
- [9] A. Rezaei Mokarram, A. Kebriaee Zadeh, M. Keshavarz, A. Ahmadi, B. Mohtat, *DARU J. Pharm. Sci.* **2010**, *18*, 185–92.
- [10] K. Gong, R. Viboonkiat, I. U. Rehman, G. Buckton, J. A. Darr, *J. Pharm. Sci.* **2005**, *94*, 2583–2590.
- [11] G. Van Den Mooter, D. Q. M. Craig, P. G. Royall, *J. Pharm. Sci.* **2001**, *90*, 996–1003.
- [12] M. Yoshioka, C. Bruno, B. C. Hancock, G. Zografi, *J. Pharm. Sci.* **1995**, *84*, 983–986.
- [13] D. Mcnamara, S. Yin, D. Pan, G. Crull, P. Timmins, B. Vig, *Mol. Pharm.* **2017**, *14*, 377–385.
- [14] Y. Song, X. Yang, X. Chen, H. Nie, S. Byrn, J. W. Lubach, *Mol. Pharm.* **2015**, *12*, 857–866.
- [15] D. Law, E. A. Schmitt, K. C. Marsh, E. A. Everitt, W. Wang, J. J. Fort, S. L. Krill, Y. Qiu, *J. Pharm. Sci.* **2004**, *93*, 563–570.
- [16] D. S. Jones, Y. Tian, S. Li, T. Yu, O. A. Abu-Diak, G. P. Andrews, *J. Pharm. Sci.* **2016**, *105*, 3064–3072.
- [17] P. Gupta, V. K. Kakumanu, A. K. Bansal, *Pharm. Res.* **2004**, *21*, 1762–1769.
- [18] K. Lehmkeper, S. O. Kyeremateng, O. Heinzerling, M. Degenhardt, G. Sadowski, *Mol. Pharm.* **2017**, *14*, 157–171.
- [19] J. C. Dinunzio, J. R. Hughey, C. Brough, D. A. Miller, R. O. Williams, J. W. McGinity, *Drug Dev. Ind. Pharm.* **2010**, *36*, 1064–1078.
- [20] F. Tanno, Y. Nishiyama, H. Kokubo, S. Obara, *Drug Dev. Ind. Pharm.* **2004**, *30*, 9–17.
- [21] D. T. Friesen, R. Shanker, M. Crew, D. T. Smithey, W. J. Curatolo, J. A. S.

- Nightingale, *Mol. Pharm.* **2008**, *5*, 1003–1019.
- [22] K. Lehmkemper, S. O. Kyeremateng, O. Heinzerling, M. Degenhardt, G. Sadowski, *Mol. Pharm.* **2017**, *14*, 4374–4386.
- [23] Y. Ishizuka, K. Ueda, H. Okada, J. Takeda, M. Karashima, K. Yazawa, K. Higashi, K. Kawakami, Y. Ikeda, K. Moribe, *Mol. Pharm.* **2019**, *16*, 2785–2794.
- [24] X. Lu, C. Huang, M. B. Lowinger, F. Yang, W. Xu, C. D. Brown, D. Hesk, A. Koynov, L. Schenck, Y. Su, *Mol. Pharm.* **2019**, *16*, 2579–2589.
- [25] Dow Chemical Co., *AFFINISOL™ HPMCAS for Spray-Dried Dispersion (SDD)*, **2014**.
- [26] Ashland, *AQUASOLVE™. Physical and Chemical Properties Handbook*, **2016**.
- [27] ShinEtsu Co., *Hypromellose Acetate Succinate Shin-Etus AQOAT*, **2005**.
- [28] *NMR in Pharmaceutical Sciences*, (Eds: J. R. Everett, R. K. Harris, J. C. Lindon), John Wiley & Sons Ltd, **2015**.
- [29] *NMR Spectroscopy in Pharmaceutical Analysis*, (Eds: U. Holzgrabe, I. Wawer, B. Diehl), Elsevier Science, **2008**.
- [30] M. Pellecchia, I. Bertini, D. Cowburn, C. Dalvit, E. Giralt, W. Jahnke, T. L. James, S. W. Homans, H. Kessler, C. Luchinat, et al., *Nat. Rev. Drug Discov.* **2008**, *7*, 738–745.
- [31] D. M. Sperger, E. J. Munson, *AAPS PharmSciTech* **2011**, *12*, 821–833.
- [32] R. K. Harris, *J. Pharm. Pharmacol.* **2007**, *59*, 225–239.
- [33] A. Paudel, M. Geppi, G. Van Den Mooter, *J. Pharm. Sci.* **2014**, *103*, 2635–2662.
- [34] A. S. Tatton, T. N. Pham, F. G. Vogt, D. Iuga, A. J. Edwards, S. P. Brown, *Mol. Pharm.* **2013**, *10*, 999–1007.
- [35] M. Toba, J. Brown, A. B. Dennis, M. Fakes, Q. I. Gao, J. Gamble, Y. Z. Khimyak, G. McGeorge, C. Patel, W. Sinclair, et al., *J. Pharm. Sci.* **2009**, *98*, 3456–3468.
- [36] Y. Song, D. Zemlyanov, X. Chen, H. Nie, Z. Su, K. Fang, X. Yang, D. Smith, S. Byrn, J. W. Lubach, *Mol. Pharm.* **2016**, *13*, 483–492.
- [37] D. M. Pisklak, M. A. Zielińska-Pisklak, Ł. Szeleszczuk, I. Wawer, *J. Pharm. Biomed. Anal.* **2016**, *122*, 81–89.
- [38] O. Petermann, M. Brackhagen, M. Sprehe, R. B. Appell, *Eur. Pat. Off.* **2018**, EP2964679B.
- [39] B. M. Fung, A. K. Khitrin, K. Ermolaev, *J. Magn. Reson.* **2000**, *142*, 97–101.
- [40] D. C. Apperley, R. K. Harris, P. Hodgkinson, *Solid-State NMR. Basic Principle & Practice*, Momentum Press, LLC, **2012**.
- [41] R. R. Ernst, G. Bodenhausen, A. Wokaun, *Principles of Nuclear Magnetic Resonance in One and Two Dimensions*, Oxford Science Publications, **1990**.
- [42] X. Wu, S. T. Burns, K. W. Zilm, *J. Magn. Reson. A* **1994**, *111*, 29–36.

- [43] C. R. Morcombe, K. W. Zilm, *J. Magn. Reson.* **2003**, *162*, 479–486.
- [44] Y. Onda, H. Muto, K. Maruyama, *U.S. Pat.* **1978**, *US4226981A*.
- [45] A. Idström, S. Schantz, J. Sundberg, B. F. Chmelka, P. Gatenholm, L. Nordstierna, *Carbohydr. Polym.* **2016**, *151*, 480–487.
- [46] H. Kono, S. Yunoki, T. Shikano, M. Fujiwara, T. Erata, M. Takai, *J. Am. Chem. Soc.* **2002**, *124*, 7506–7511.
- [47] H. Yang, T. Wang, D. Oehme, L. Petridis, M. Hong, J. D. Kubicki, *Cellulose* **2018**, *25*, 23–36.
- [48] J. Xu, R. Y. Dong, V. Domenici, C. A. Veracini, *J. Phys. Chem. B* **2006**, *110*, 9434–9441.
- [49] R. M. Silverstein, F. X. Webster, D. J. Kiemle, D. L. Bryce, *Spectrometric Identification of Organic Compounds. 8th Edition*, **2005**.
- [50] P. L. Nasatto, F. Pignon, J. L. M. Silveira, M. E. R. Duarte, M. D. Nosedá, M. Rinaudo, *Polymers (Basel)*. **2015**, *7*, 777–803.
- [51] Y. Y. Chen, S. Y. Luo, S. C. Hung, S. I. Chan, D. L. M. Tzou, *Carbohydr. Res.* **2005**, *340*, 723–729.
- [52] S. Warashina, **2019**, Personal Communication.